

## ANALYSIS OF PERFORMANCE OF SCALAR LIMITERS IN HIGH-ORDER SCHEMES USED FOR UNSTRUCTURED-GRID GASDYNAMIC FLOW COMPUTATIONS

E.V. Kolesnik<sup>1\*</sup>, E.M. Smirnov<sup>1</sup>

<sup>1</sup>Department of Fluid Dynamics, Combustion and Heat Transfer, Peter the Great St.-Petersburg Polytechnic University, Saint-Petersburg, Russia

**Abstract.** Several high-order schemes used for unstructured-grid gas dynamic flow computations are described. The Roe's approximate Riemann solver is used for evaluation of the numerical fluxes at finite-volume faces. The MUSCL approach added by introducing a scalar limiter is used in order to achieve higher-order spatial approximation. Comparative analysis of performance of different limiters suggested in the literature is carried out via computations of transonic 2D in viscid flow past the NACA-0012 airfoil.

**Keywords:** compressible flow, numerical simulation, MUSCL approach, unstructured grid, scalar limiter.

**AMS Subject Classification:** 76H05, 65Z05.

**Corresponding Author:** Kolesnik Elizaveta, Department of Fluid Dynamics, Combustion and Heat Transfer, Peter the Great St.-Petersburg Polytechnic University, Politechnicheskaya str., 29, 195251, Saint-Petersburg, Russia, e-mail: [kolesnik\\_ev@mail.ru](mailto:kolesnik_ev@mail.ru)

**Manuscript received:** 8 July 2017

### 1. Introduction

Transonic and supersonic flows may contain gas dynamic discontinuities; therefore special approaches in their numerical simulation are required. The main issue is how to approximate convective fluxes. Numerical scheme for convective flux evaluation should provide sufficiently accurate resolution of discontinuities in the absence of the spurious oscillations caused by solution discontinuities. Godunov-type schemes, based on solving the local Riemann problem for a computational cell interface, satisfy these requirements, for example, the Roe scheme [8]. In its basic form, any Godunov-type scheme is of the first-order accuracy, since it is constructed under assumption of the piecewise-constant approximation of the solution. Higher order spatial discretization can be achieved by replacing the piece-wise-constant approximation of the solution by a piecewise-polynomial approximation for each cell, in particular by a piecewise-linear approximation in the case of second-order scheme. This technique is known as the MUSCL approach [10], and its primary role is to provide reconstructed values of gas-dynamic variables at the "left" and 'right' sides of a cell interface. Remarkably, that the stage of variable reconstruction is completely decoupled from the physical stage that covers solving the Riemann problems all the cell interfaces. However, the use of high-order schemes may lead to appearance of

spurious numerical oscillations around discontinuities. To avoid or at least to diminish considerably such deficiencies of the solution a special non-linear limiter-function should be used at the polynomial reconstruction stage in order to modify properly slope of the solution in each cell.

Most methods of limiter-based control of the oscillations are based on consideration of the one-dimensional scalar conservation equation. For this case, a reliable theory of non-oscillatory schemes has been developed [2, 3]. In the case of structured grids, these schemes can be extended to multidimensional problems in a straightforward way, using the quasi-one-dimensional approach. In the case of unstructured grids, there are two main techniques for variable reconstruction and limiter formulation. The first way is generalization of the quasi-one-dimensional approach that is applied locally for each current face of an unstructured-grid cell (finite-volume). Methods of the second group are initially developed for multidimensional unstructured-grid applications, in these methods a scalar limiter-function is calculated using values of appropriate gas-dynamic variables in all neighbors' finite volumes.

Starting from the pioneering work of Barth and Jespersen [1], the multidimensional approach was under active subsequent developments [5, 7, 11]. Some authors [5-7] have proposed also to use a second limiter that is a special function, which controls area where the main (primary) limiter is active.

Despite a big amount of publications on the matter, there is no common opinion on the efficiency of a particular scalar limiter formulation for higher-order accuracy unstructured-grid computations. The present work is aimed at a comparative testing of different schemes with scalar limiters.

## 2. Computational Method

### 2.1. General formulation of the finite volume method

Balance equations for compressible gas flows in a finite-volume formulation can be written as:

$$\int_{\Omega} \frac{\partial \vec{w}}{\partial \tau} d\Omega + \sum_M \int_{S_m} \vec{F} dS = 0, \quad (1)$$

where  $\Omega$  is the control (finite) volume,  $M$  – number of finite-volume faces,  $S_m$  – area of the current face,  $m=1, M$ ,  $\vec{w} = [\rho, \rho u, \rho v, \rho w, \rho H]$  – vector of variables,  $\vec{F} = [\rho V_n, \rho u V_n + p n_x, \rho v V_n + p n_y, \rho w V_n + p n_z, \rho H V_n]$  – flux vector,  $n_x, n_y, n_z$  – components of the normal to the face.

Convective flux at a finite volume face can be written as a sum of the central-scheme flux and a diffusive flux:  $\vec{F}_f = \langle \vec{F} \rangle - \vec{D}$ . In the first-order scheme the central-scheme flux is calculated as an average of values for the neighboring (“left” and “right”) computational cells (control volumes), the diffusive flux is evaluated by using the Roe’s approximate Riemann solver:

$$\begin{aligned}\langle \bar{F} \rangle &= \frac{1}{2}(\bar{F}(\bar{w}^R) - \bar{F}(\bar{w}^L)) \\ \bar{D} &= \frac{1}{2}|\tilde{A}(\bar{w}^R, \bar{w}^L)|(\bar{w}^R - \bar{w}^L)\end{aligned}\quad (2)$$

Jacobian  $\tilde{A} = (\partial \bar{F} / \partial \bar{w})$  on the face is calculated with the Roe's average values of variables:

$$\begin{aligned}\tilde{\rho} &= \sqrt{\rho_R \rho_L} \\ \tilde{V} &= (\sqrt{\rho_R} \vec{V}_R + \sqrt{\rho_L} \vec{V}_L) / (\sqrt{\rho_R} + \sqrt{\rho_L}) \\ \tilde{H} &= (\sqrt{\rho_R} H_R + \sqrt{\rho_L} H_L) / (\sqrt{\rho_R} + \sqrt{\rho_L})\end{aligned}\quad (3)$$

In case of second-order schemes, the central-scheme flux and the diffusive one are written as:

$$\begin{aligned}\langle \bar{F} \rangle &= 0.5(\bar{F}(\bar{w}_f^L) + \bar{F}(\bar{w}_f^R)), \\ \bar{D} &= \frac{1}{2}|\tilde{A}(\bar{w}_f^R, \bar{w}_f^L)|(\bar{w}_f^R - \bar{w}_f^L),\end{aligned}\quad (4)$$

where  $\bar{w}_f^{L/R}$  denotes results of piecewise-linear reconstruction of the solution in the left/right cells.

## 2.2. Solution reconstruction and limiters

Piecewise-linear reconstruction of the solution in each cell is performed using gradients of involved variables at the cell center. For a current face, it gives

$$u_f^{L/R} = u^{L/R} + \varphi_{L/R}(\nabla u)_{L/R} \cdot \vec{r}_{L/R}, \quad (5)$$

where  $u$  stands for any of the variables involved,  $\varphi_{L/R}$  – value of the scalar limiter in the left/right cell,  $\vec{r}_{L/R}$  – vector from the left/right cell center to the face center.

Let's give formulations for several variants of the limiters presented in the literature, as well as for groups of limiters, for the sake of brevity, also called limiters.

**Variant 1.** In [1], a scalar limiter (termed below as the BJ limiter) was proposed, the formulation of which is based on the monotonicity principle declaring that values of the linearly reconstructed function must not exceed the maximum and minimum of neighboring centroid values. The values of the limiter for each cell are found by the following procedure:

1. Find the largest negative and positive difference between the solution in the immediate neighbors (index  $j$ ) and the current control volume (index  $i$ )

$$\delta u^{min/max} = \min/\max(u_j - u_i) \quad (6)$$

2. Compute the unconstrained reconstructed value at each face:

$$u_{ij} = u_i + (\nabla u)_i \cdot \vec{r}_{ij} \quad (7)$$

3. Compute a maximum allowable value of  $\varphi_{ij}$  for all faces:

$$\varphi_{ij} = \Phi(y) = \min(1, y), \tag{8}$$

where  $y = \Delta_+ / \Delta_-$ ,  $\Delta_- = u_{ij} - u_i$ ,  $\Delta_+ = \delta u^{max}$  if  $\Delta_- > 0$ ,  $\Delta_+ = \delta u^{min}$  if  $\Delta_- < 0$ ,  $\varphi_{ij} = 1$  if  $\Delta_- = 0$ .

4. Calculate minimum value of  $\varphi_{ij}$  :

$$\varphi_i = \min(\varphi_{ij}) \tag{9}$$

Variant 2. According to the numerous evidence in the literature, usage of the BJ limiter may adversely affect the convergence properties of the solver. This happens for two reasons: non-differentiability in the computation of the reconstructed function and applying the limiter in regions of nearly uniform flow.

Venkatakrishnan [11] has suggested several modification of the BJ limiter. He has introduced a smooth alternative to step 3 of the Barth-Jespersen procedure by replacing the function  $\Phi(y) = \min(1, y)$  with  $\Phi(y) = (y^2 + 2y) / (y^2 + y + 2)$  (Fig.1 (c)). A further modification has been made to avoid applying the limiter in regions of nearly uniform flow and smooth extreme. Eliminating the effect of the limiter when  $u_{ij} - u_i < \varepsilon$ , where  $\varepsilon = (K\Delta x)^{3/2}$ ,  $\Delta x$  is a characteristic length for the control-volume and  $K$  is a tunable parameter, is achieved by adding a threshold to the function  $\Phi(y)$ . As a result, (8) is replaced by following:

$$\varphi_{ij} = \frac{1}{\Delta_-} \left[ \frac{(\Delta_+^2 + \varepsilon^2)\Delta_- + 2\Delta_-^2\Delta_+}{\Delta_+^2 + 2\Delta_-^2 + \Delta_+\Delta_- + \varepsilon^2} \right]. \tag{10}$$

Variant 3. In [5, 6] other modifications of the BJ limiter are presented. Firstly, a new approximation for  $\Phi(y)$ , instead of  $\min(1, y)$ , is proposed:

$$\Phi(y) = \begin{cases} P(y), & y < y_t \\ 1, & y > y_t \end{cases}, \tag{11}$$

where  $1 < y_t < 2$ ,  $P(y)$  is the cubic polynomial satisfying  $P(0) = 0$ ,  $P(y_t) = 1$ ,  $dP/dy(0) = 1$ ,  $dP/dy(y_t) = 0$  (Fig.1 (c)).

Secondly, eliminating the effect of the limiter in nearly uniform regions is achieved by using the “second” limiter, which “switches off” the primary limiter when  $\delta u = \delta u^{max} - \delta u^{min} < (K\Delta x)^{3/2}$ , where  $\Delta x$  is a characteristic length of the control-volume. Besides, the “third” limiter, based on Mach-number distribution, is used to prevent the application of the limiter at stagnation points.

Variant 4. The BJ limiter modifications suggested in [5, 6] require assignment of appropriate values of several user-specified parameters that is not convenient for engineering practice. In [4], a new second limiter has been proposed, which is simple, parameter-free, and easy-to-use:

$$\begin{aligned} \varphi_2 &= \max[\varphi_1, F(M_{max})], \\ F(M) &= 0.5\{1 - \tanh(L\pi(M - 1))\}, \end{aligned} \tag{12}$$

where  $M_{\max}$  is maximum Mach number in neighboring volumes,  $\phi_1$  is any primary slope limiters, in particular the BJ limiter,  $L$  is a parameter, (its recommended value is of 5.0 [4]).

**Variant 5.** The limiter introduced in [7] takes into account more multi-dimensional flow physics, involving values of variables both in the cell-centers and the vertices surrounding or belonging to the cell of interest. For each current vertex, indexed by  $q$ , maximum allowable value of  $\phi_q$  is computed as:

$$\phi_q = \Phi(y) = \min(1, y), \tag{13}$$

where  $y = \Delta_+ / \Delta_-$ ,  $\Delta_- = \nabla u_i \cdot \vec{r}_q$ ,  $\Delta_+ = u_q^{\max} - u_i$  if  $\Delta_- > 0$ ,  $\Delta_+ = u_q^{\min} - u_i$  if  $\Delta_- < 0$ ,  $\phi_q = 1$  if  $\Delta_- = 0$ ,  $u_q^{\min/\max}$  – minimum/maximum value among those for all the neighboring volumes which share the vertex  $q$ ,  $\vec{r}_q$  vector from the cell center to vertex  $q$ . Then the minimum value among the all found for  $\phi_q$  are selected.

**Variant 6.** In the same work [7], modifications of the primary limiter similar to those proposed in [11] were presented as well. According to these modifications, for each vertex  $q$  maximum allowable value of  $\phi_q$  is computed by using formula (10) instead of (9), where  $\Delta_+$  and  $\Delta_-$  are defined as in variant 5.

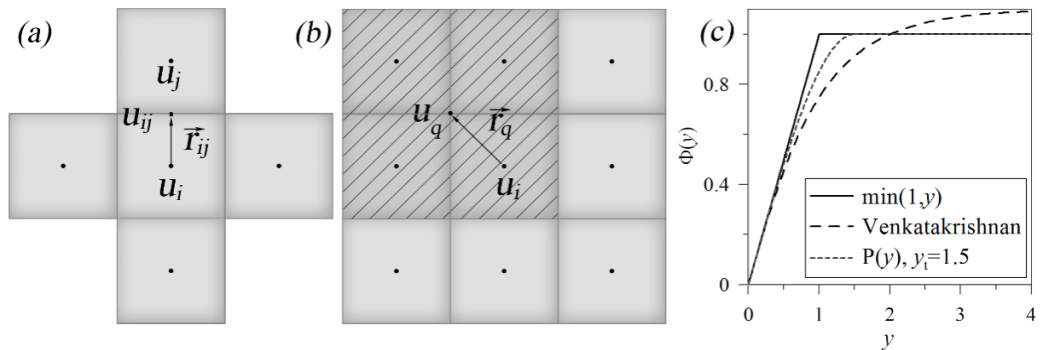


**Fig. 1.** Scheme to Construction of limiters (a,b) and variants of function  $\Phi(y)$  (c)

Short denotations of the limiters under consideration are given in Table 1. The parentheses in some positions cover parameters of corresponding limiters. Parameters  $M_1$  and  $M_2$  of the MO limiter were introduced in [6], and the values recommended in [6] were assigned for these parameters when performing computations presented below.

Table 1.Limiter denotation

Limiter	denotation
Variant 1 [1]	BJ
Variant 2 [11]	VK ( $K$ )
Variant 3 [5, 6]	MO ( $K, M_1, M_2$ )
Variant 4 [4]	KS ( $L$ )

Variant 5 [7]	MLP- $u_1$
Variant 6 [7]	MLP- $u_2(K)$

### 3. Results and discussion

The in-house CFD-code SINF [9] that is under permanent development at the St.-Petersburg Polytechnic University was used for the present computations. All the above given second-order schemes have been implemented in the code. Linear-reconstruction procedure is applied to conservative variables, and the Green-Gauss method is used for gradient calculations. The time-stepping is carried out with an implicit scheme introducing increments of variables. Discretization of the implicit (“stabilizing”) operator is based on the first-order split coefficient matrix method.

Comparative test computations varying limiters have been carried out considering 2D problems of inviscid gas flow. In the present work, results obtained for transonic flow over a NACA 0012 airfoil with free-stream Mach number of 0.8 and angle of attack 1.25 degrees (Fig. 2(a)) are reported. The solutions given below were obtained with a computational mesh consisting of  $161 \times 42$  nodes (Fig. 2(b)), the Courant number was set to 0.2. These solutions are compared with the grid-converged (reference) solution (Fig.2 (c)) calculated with the second-order SLIP scheme [4], also implemented in the SINF code.

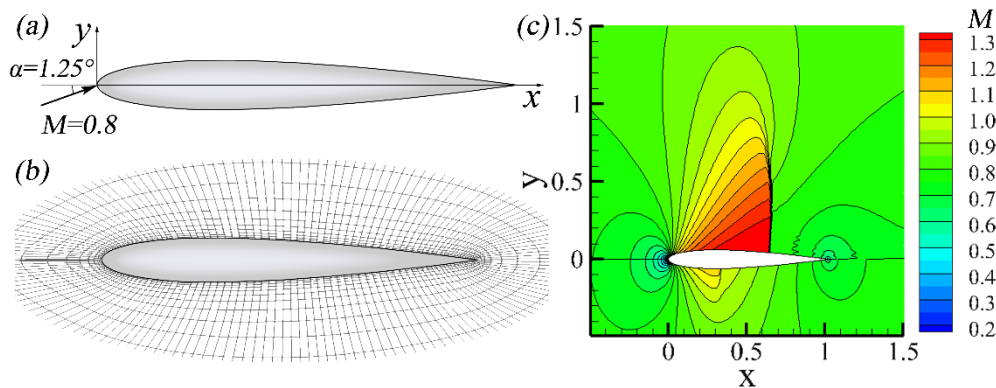


**Fig. 2.** Scheme of flow past NACA-0012 airfoil (a), fragment of computational mesh (b) and Mach number map for reference solution (c)

Fig. 3 presents a comparison of the airfoil-surface pressure coefficient distributions computed with different schemes/limiters. Namely, zones near the suction-side shock and in the vicinity of the leading edge are shown. One can see that all the limiters are effective with respect to eliminating un-physical oscillations in the shock region.

It should be noted however that usage of the BJ and the MLP- $u_1$  limiters causes difficulties in getting a fully-converged steady-state solution: convergence stalls after about two-three orders of magnitude reduction in the maximal residuals. Limiters VK(0) and MO(0,0,0) also fail to reach full convergence, despite the use of differentiable functions in their formulation. Fully converged

solutions were obtained with the MO(3, 0.8, 0.85), VK(3), KS(1), MLP-u<sub>2</sub>(3) limiters when selecting appropriate values of the parameters to avoid applying the limiter in regions of nearly uniform flow.

The solution closest to the reference one is obtained in the case of the BJ scheme, in spite of the lack of full convergence. The solution computed with the VK (0) limiter deviates more from the reference one in the near-leading-edge region. It is attributed to the fact that the function  $\Phi(y)$  given by (10) lies substantially below the function  $\min(1,y)$  for small values of  $y$  (see Fig. 1 (c)). Adding a threshold to the function  $\Phi(y)$  that corresponds to the limiter VK (3) case allows to remedy this drawback. The solution obtained with the MO(0,0,0) limiter practically does not differ from the BJ limiter solution.

Fig.4 shows spatial distributions of the limiter under testing (for variable  $\rho$ ). One can see that in case of the MLP limiter the zone where the limiter is activated is much larger than for other variants. The MLP-u<sub>2</sub>(3) limiter is activated near the leading edge, because of that the solution deviates more from the reference one even when using the threshold suggested. Applying the KS limiter is quite efficient for this test case, however it is not applicable to pure supersonic flows.

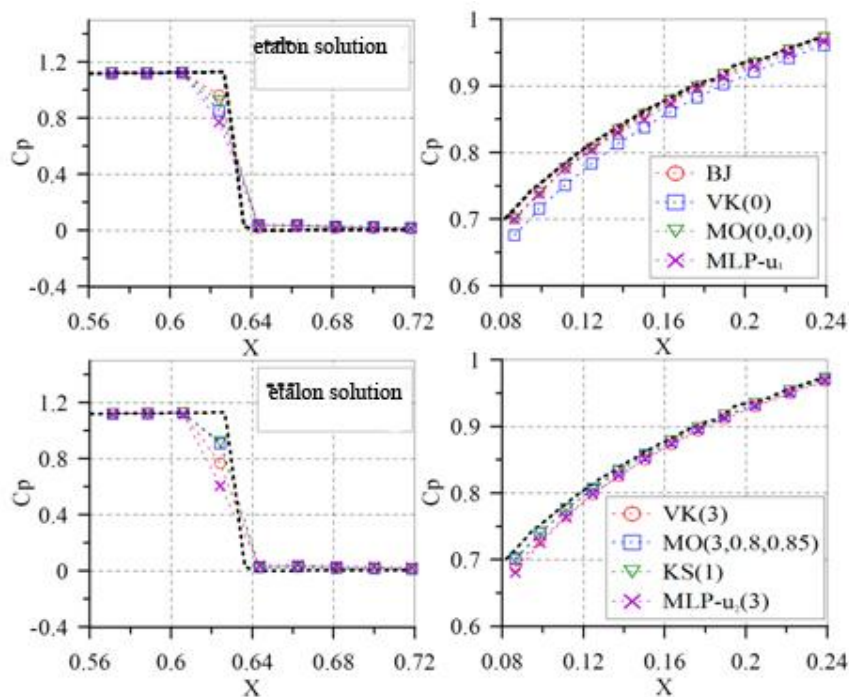


**Fig. 3.** Computed surface pressure variations in the shock region (left) and near the leading edge (right)

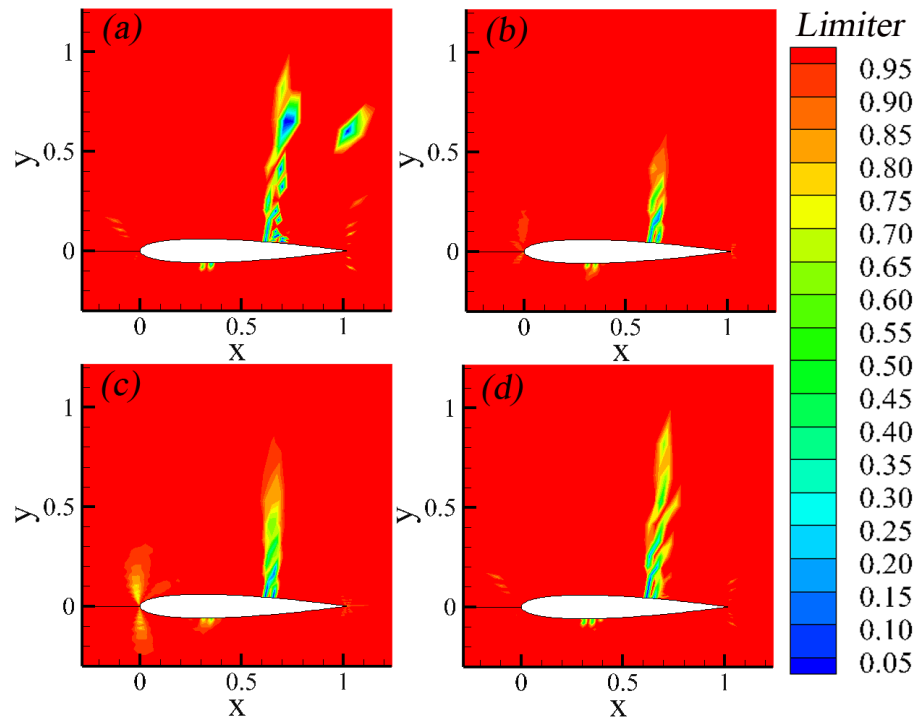


Fig. 4. Maps of limiter values: BJ (a); VK(3) (b); MLP-u2(3) (c); KS(1) (d)

### 3. Conclusion

Slope limiters can cause convergence problems when computing gas dynamic flows with discontinuities. As a result of the fulfilled testing of various formulations of the limiters reported in the literature, problematic variants have been distinguished, especially those when one is not able to get a fully converged solution.

Fully converged solutions can be obtained with the use of fully differentiable limiters which are not activated in the regions of nearly uniform flow. However, usage of differentiable functions may lead to additional numerical dissipation. The smallest amount of dissipation is achieved when using a smooth limiter function  $\Phi(y)$  which lies closest to  $\min(1, y)$ , as in the case of the MO limiter. Eliminating the limiter effects in zones of nearly uniform flow requires additional efforts to select optimal values of parameters used in the primary, the second and, if any, third limiters.

### References

1. Barth, T.J., Jespersen, D.C. (1989). The design and application of upwind schemes on unstructured meshes. *AIAA Paper*, No.89-0366.
2. Harten, A. (1983). High resolution schemes for hyperbolic conservation laws. *J. Comput. Phys.*, 49(3), 357-393.
3. Jameson, A. (1993). Artificial diffusion, upwind biasing, limiters and their effect on accuracy and multigrid convergence in transonic and hypersonic flow. *AIAA Paper*, No. 93-3359.

4. Kitamura, K., Shima, E. (2012). Simple and parameter-free second slope limiter for unstructured grid aerodynamic simulations. *AIAA journal*, 50(6), 1415-1426.
5. Michalak, K., Ollivier-Gooch, C. (2008). Limiters for unstructured higher-order accurate solutions of the Euler equations. In: *Proceedings of the AIAA Forty-Sixth Aerospace Sciences Meeting*, 2008.
6. Michalak, K., Ollivier-Gooch, C. (2009). Accuracy preserving limiter for the high-order accurate solution of the Euler equations. *J. Comput. Phys.*, 228, 8693-8711.
7. Park, J.S., Yoon, S.H., Kim, C., (2010). Multi-dimensional limiting process for hyperbolic conservation laws on unstructured grids. *J. Comput. Phys.*, 229, 788-812.
8. Roe, P.L. (1981). Approximate Riemann Solvers, parameter vectors, and difference schemes. *J. Comput. Phys.*, 43(2), 357-372.
9. Smirnov, E.M., Zaytsev, D.K. (2004). Finite volume method as applied to hydro-and gas dynamics and heat transfer problems in complex geometry domains, *St. Petersburg State Polytechnic University Journal, Physics and Mathematics*, 2(36), 70-81.
10. Van Leer, B., (1979). Towards the ultimate conservative difference scheme. V.A second order sequel to Godunov's method. *J. Comput. Phys.*, 32(1), 101-136.
11. Venkatakrishnan, V., (1995). Convergence to steady state solutions of the Euler equations on unstructured grids with limiters. *J. Comput. Phys.*, 118, 120-130.